Proceedings of ASME Turbo Expo 2014: Turbine Technical Conference and Exposition
GT2014
June 16 – 20, 2014, Düsseldorf, Germany

GT2014-25753

AN EFFICIENT COMPONENT MAP GENERATION METHOD FOR PREDICTION OF GAS TURBINE PERFORMANCE

Elias Tsoutsanis, Nader Meskin, Mohieddine Benammar
Department of Electrical Engineering
College of Engineering
Qatar University
Doha, Qatar
Email: [elias.tsoutsanis, nader.meskin, mbenammar]@qu.edu.qa

Khashayar Khorasani
Department of Electrical and
Computer Engineering
Concordia University
Montreal, Canada
Email: kash@ece.concordia.ca

ABSTRACT

Improving efficiency, reliability and availability of gas turbines have become more than ever one of the main areas of interest in gas turbine research. This is mainly due to the stringent environmental regulations that have to be met in such a mature technology sector; and consequently new research challenges have been identified. One of these involves the establishment of high fidelity, accurate, and computationally efficient engine performance simulation, diagnosis and prognosis technology.

Performance prediction of gas turbines is strongly dependent on detailed understanding of the engine component behaviour. Compressors are of special interest because they can generate all sorts of operability problems like surge, stall and flutter; and their operating line is determined by the turbine characteristic. Compressor performance maps, which are obtained in costly rig tests and remain manufacturers proprietary information, impose a stringent limitation that has been commonly resolved by scaling default generic maps in order to match the targeted off-design or engine degraded measurements. This approach is efficient in small range of operating conditions but becomes less accurate for a wider range of operations.

In this paper, a novel compressor map generation method, with the primary objective of improving the accuracy and fidelity of the engine model performance prediction is developed and presented. A new compressor map fitting and modelling method is introduced to simultaneously determine the best elliptical curves to a set of compressor map data. The coefficients that determine the shape of compressor maps' curves have been analyzed and tuned through a multi-objective optimization algorithm in order to meet the targeted set of measurements. The proposed component map generation method is developed in the object oriented Matlab/Simulink environment and is integrated in a dynamic gas turbine engine model. The accuracy of this method is evaluated for off-design steady state and transient engine conditions. The proposed compressor map generation method has the capability to refine current gas turbine performance prediction approaches and to improve model-based diagnostic techniques.

NOMENCLATURE

Latin

A	matrix of elements α
N	corrected shaft rotational speed
P	pressure (Pa)
T	temperature (K)
W	actual mass flow rate (kg/s)
$\mathbf{X}$	component characteristics vector
$\mathbf{Y}$	measurement vector
a	semi-major axis of ellipse
b	semi-minor axis of ellipse
f	flow rate (kg/s)
g	generic form of map's sub/coefficients
m	corrected mass flow rate
n	total number of operating points per speed line

q total number of speed lines
$\mathbf{u}$ ambient and operating conditions vector
x coordinate of ellipse in x-axis
y coordinate of ellipse in y-axis

Greek
α element of matrix A
η isentropic efficiency
θ angle of rotated ellipse (deg)
π pressure ratio

Subscript
c compressor
des design point
f fuel
i order of polynomial, number of speedlines
j number of operating points
r reference engine
0 not rotated coordinate, θ=0
2 compressor inlet
3 compressor exit
4 combustor exit
5 turbine exit
6 power turbine exit

1 INTRODUCTION

Gas turbine performance simulation, diagnosis and prognosis are strongly dependent on detailed understanding of the engine component behavior. Especially at off-design conditions of the gas turbine the quality of the engine's component maps is crucial for the accuracy of the prediction. Compressors are of special interest because they can generate all sorts of operability problems like surge, stall and flutter; and their operating line is determined by the turbine characteristic. The shape of the maps determines the values of measurable parameters at off-design operating conditions. Compressor maps are Original Equipment Manufacturer's (OEM) design information since they are the outcome of costly rig tests. Maps can also be calculated by Computational Fluid Dynamics (CFD), if the geometry of the compressor is known, or other calibrated methods. Gas turbine users do not have access in the context of such maps and are only limited to use the tailored to customer deck for performance calculations. The above limitations have motivated gas turbine research community to explore alternative methods of representing the compressor map in order to improve the accuracy of the performance prediction.

A generalized compressor map developed by Saravanamuttoo and Mac Isaac [1] has been used by Zhu and Saravanamuttoo [2] for off-design performance simulation. Kurzke [3] introduced auxiliary coordinates (beta lines), having no physical meaning, which are superimposed, in order to address the non-uniqueness and ill-conditioning issues of the compressor map shapes. Miste and Benini [4] defined a bivariate b-function used for interpolation of the compressor maps and optimization for minimizing interpolation errors. Jones *et al.* [5] and Sethi *et al.* [6] introduced quasi-physics-based backbone compressor mapping approaches.

The most commonly used method involves scaling and shifting the shape of a similar compressor map through optimization such that it matches the targeted engine measurements. Such a scaling method was proposed by Kong *et al.* [7] on the condition that the initial map has a very similar shape to the actual map. In case that the compressor map used in the engine model is not similar to the one of the actual engine, nonlinear effects of the gas turbine behavior at off-design conditions cannot be captured accurately. This is because the scaling coefficients reconstruct the shape of the compressor map linearly so every point on the map is multiplied by a single set of constant coefficients. Recently Li *et al.* [8] suggested a unique set of scaling coefficients for each line of constant speed and efficiency to capture these nonlinear effects. A combined hybrid approach developed by Kong *et al.* [9] takes advantage of genetic algorithms to determine the coefficients of the polynomial equations of the system identification method. This method provides higher accuracy than the traditional scaling methods at operating points far away from the design point of the engine.

The work by Drummond and Davison [10] examined the shape variance of the compressor maps for a wide range of compressor shapes and related them to the physical processes. Sieros *et al.* [11] proposed the concept of analytically expressing the compressor maps as a function of speed and mass flow in order to account for the nonlinear behaviour of the engine and implementing the process for adaptation and diagnosis. An alternative mathematical approach was studied by Tsoutsanis *et al.* [12] and successfully applied [13] to match off-design test data of an industrial gas turbine operating in a combined cycle power plant. Other approaches which are based on the input and output relationship for the engine/component performance with the use of neural networks have been developed by Yu *et al.* [14], and M. Gholamrezaei and K. Ghorbanian [15]. The accuracy of these methods depends on the quality and quantity of engine data either from the engine manufacturer or the engine user.

Although the benefits of the above approaches for engine performance prediction are extensive, trade-offs between key parameters such as the operating range, accuracy, complexity and computation time are still debated. It is essential to develop a robust, mathematically proven, generic and computationally efficient approach for predicting a gas turbine's performance by satisfying multiple set of measurements from the off-design steady state and transient conditions.

In this paper, an efficient compressor map generation method for improving the accuracy of the gas turbine performance prediction is developed as explained in Section 2. Op-

posed to the earlier study [12], where the shape of a compressor map was expressed by the mathematical equations of an ellipse with fixed center and no rotation, this study proposes an advanced and a more accurate approach by considering rotation of the ellipses and transformation of its coordinates. Moreover, its application is not only tested to the steady state off-design conditions [13], but also extends to transient conditions.

The proposed method has the capability to refine the current gas turbine performance adaptation and model-based diagnostic techniques, and is integrated into a dynamic engine model developed in Matlab/Simulink environment. Section 3 of the paper describes the application of this approach to a compressor map available from the literature. The results of this application are presented in Section 4 in order to clarify the former debateable trade-offs. The dynamic engine model itself and its validation against the gas turbine simulation software PROOSIS [16] were the subject of an earlier paper [17] presented by the authors. The concluding remarks drawn from this study are summarized in Section 5.

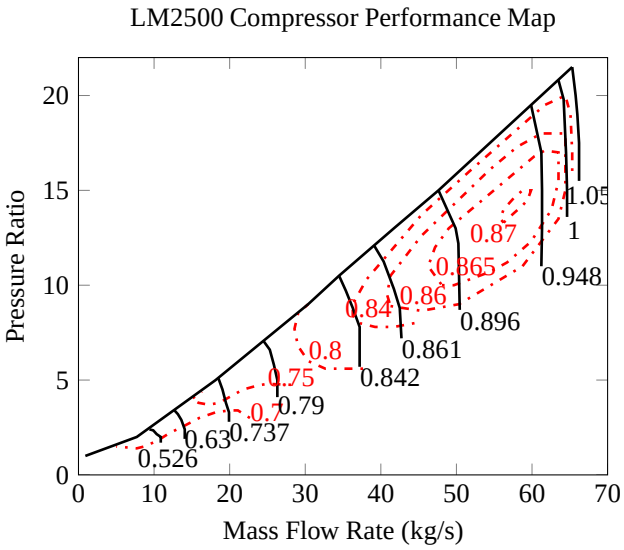

FIGURE 1: Compressor performance map reproduced from [18].

2 METHODOLOGY

Axial compressor performance maps are used in gas turbine thermodynamic models for estimation of key component performance parameters such as pressure ratio π_c, corrected mass flow rate $m_c = \left(\frac{W_2 \times \sqrt{T_2}}{P_2}\right)$ and isentropic efficiency η_c. A typical compressor map has been reproduced from [18] and shown in Fig. 1. Generating compressor maps for low speed regions, below 50% of rotational speed, is another research topic that has been addressed by other scholars [19], [5] and is beyond the scope of this study. The map is usually split into simplified maps, by determining the intersection of the efficiency contours with the speed lines in a point by point basis, as seen from Fig. 2. Therefore, pressure ratio π_c and efficiency η_c are related with corrected mass flow rate m_c for several lines of constant corrected rotational speed N.

The objective of the map generation approaches is to determine mathematical equations that could accurately capture the shape of the map by expressing the corrected mass flow rate m_c as a function of the pressure ratio π_c and the corrected rotational speed N, and efficiency η_c as a function of the corrected mass flow rate m_c and the corrected rotational speed N, i.e. $m_c = f(\pi_c, N)$ and $\eta_c = g(m_c, N)$. Another way of expressing efficiency $\eta_c = h(\pi_c, N)$ is by expressing it as a function of the pressure ratio π_c which is beneficial for high rotational speed lines, which are almost vertical. A detailed description of the proposed method follows.

2.1 Map Interpolation

The process of map interpolation commences with a reference map available either from the open literature or constructed from operational data. Having the reference compressor map,

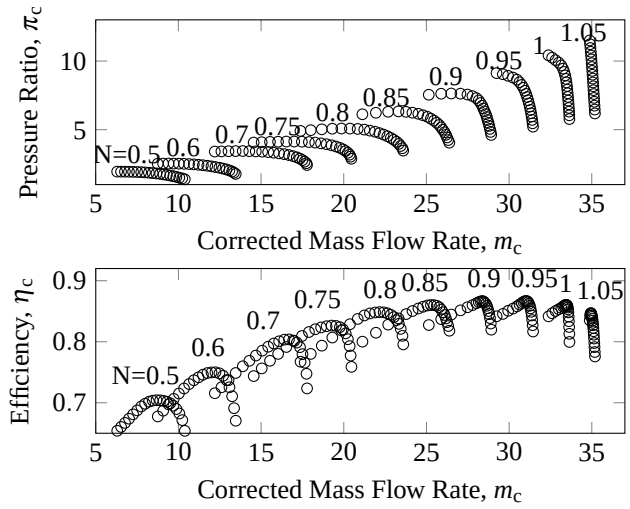

FIGURE 2: Typical compressor maps as reproduced from PROOSIS [16].

the objective is to fit the available data with a single mathematical equation, which should be of the same type for every speed line. The accuracy of the fitting procedure depends on several factors, such as the complexity of the mathematical model chosen, the quality of the data, the threshold of the tolerance criteria and the objective function that is used in the optimization, if any.

Several maps from the open literature have been used to test the validity of the proposed method but due to space limitations the work will present only the accuracy of the method applied to a compressor map available from the open literature [18], that has

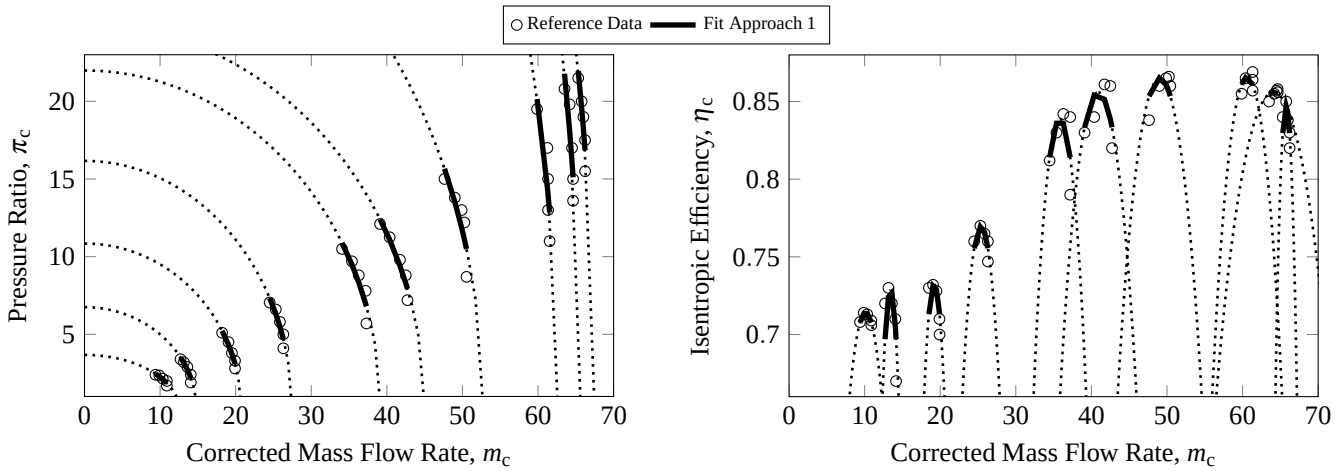

(a) π_c-Fitting Approach 1.

(b) η_c-Fitting Approach 1.

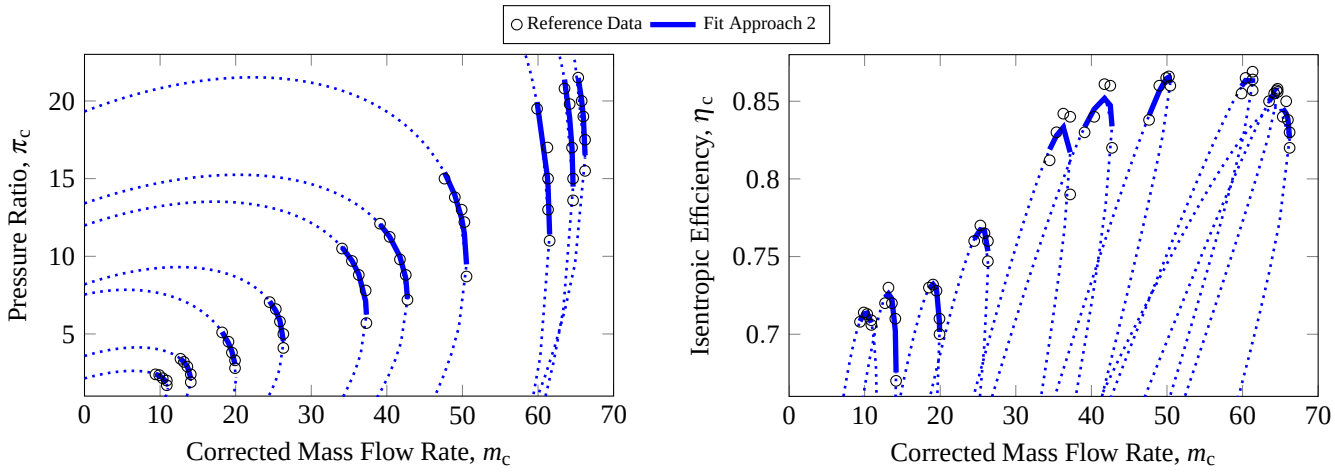

(c) π_c-Fitting Approach 2.

(d) η_c-Fitting Approach 2.

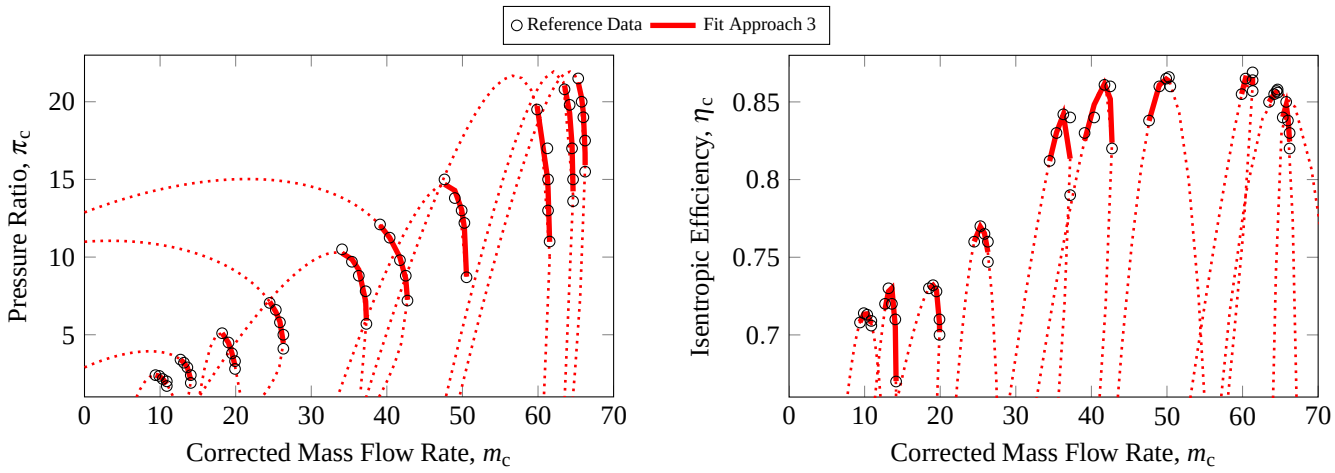

(e) π_c-Fitting Approach 3.

(f) η_c-Fitting Approach 3.

FIGURE 3: Compressor performance map fitting.

been digitized and reproduced, seen in Fig. 1. After an extensive review of several methods (polynomials, neural networks [14], [15]) for expressing the pressure ratio π_c and the efficiency η_c as a function of m_c, N, the most mathematically robust approach is determined to assume that each line belongs to an elliptic curve. The equation, adjusted for the π_c versus m_c map, is given by

$$\left(\frac{m_{c_0}-x_0}{a_{\pi_c}}\right)^2+\left(\frac{\pi_{c_0}-y_0}{b_{\pi_c}}\right)^2=1 \tag{1}$$

where a_{π_c}, b_{π_c} are the semi-major and the semi-minor axes of the ellipse, respectively, and m_{c_0}, π_{c_0} denote the values of corrected mass flow rate and pressure ratio when the ellipse is fixed at (x_0, y_0), which is the center coordinates of the ellipse. Taking into consideration that each ellipse is free to rotate, at an angle θ then the new coordinates of the ellipse (m_c, π_c) are

$$m_c = m_{c_0}\cos(\theta_{\pi_c}) - \pi_{c_0}\sin(\theta_{\pi_c}) \tag{2}$$
$$\pi_c = m_{c_0}\sin(\theta_{\pi_c}) + \pi_{c_0}\cos(\theta_{\pi_c}) \tag{3}$$

Similarly for the efficiency the governing equation is given by

$$\left(\frac{m_{c_0}-x_0}{a_{\eta_c}}\right)^2+\left(\frac{\eta_{c_0}-y_0}{b_{\eta_c}}\right)^2=1 \tag{4}$$

where a_{η_c}, b_{η_c} are the semi-minor and the semi-major axes of the ellipse, respectively, and m_{c_0}, η_{c_0} denote the values of corrected mass flow rate and efficiency when the ellipse is fixed at (x_0, y_0), which is the center coordinates of the ellipse. Once again, rotating the ellipse at an angle θ then the compressor's isentropic efficiency η_c is given by

$$\eta_c = m_{c_0}\sin(\theta_{\eta_c}) + \eta_{c_0}\cos(\theta_{\eta_c}) \tag{5}$$

where eq. (2) is used to determine m_c since the range of corrected mass flow is identical for both maps as seen in Fig. 2. The start and end of each speed line of the map generated is limited according to the variation of each coefficient w.r.t. to corrected rotational speed. A simple surge limiter, as a function of corrected rotational speed, has been implemented and does not allow the spped lines to go at lower mass flow rates.

Three approaches of different complexity have been proposed for fitting the π_c versus m_c map data with the following assumptions on the ellipses, namely

Approach 1. Center at $(0,0)$ and no rotation,
Approach 2. Center at $(0,0)$ and rotation of angle θ,
Approach 3. Center at (x_0, y_0) and rotation of angle θ.

Similar approaches are considered for the η_c versus m_c map apart from the first one, where the x_0 is assumed to be the middle point of each curve as follows:

Approach 1. Center at $(x_0, 0)$ and no rotation.
Approach 2. Center at $(0,0)$ and rotation of angle θ,
Approach 3. Center at (x_0, y_0) and rotation of angle θ.

The application of this fitting method for the selected map is shown in Fig. 3. The dashed lines of Fig. 3, which resulted from extrapolation of the curve fit outside the range of data, illustrate the shape of each ellipse. It is noticed, that the third approach is the most accurate, since there is the freedom of moving the center coordinates of the ellipsis and at the same time rotating it. The difference between the second and third approaches is not significant for both the pressure ratio and the efficiency maps.

At this point it is fundamental to evaluate, in terms of the selected optimization method, each approach since they have different complexities. The common parameters of each ellipse for all approaches are a, b. In addition, angle θ of the rotated ellipse is employed in both approaches 2 and 3. The third approach has the center coordinates (x_0, y_0) and the first approach for efficiency map has an additional one at x_0.

The above terms, which are referred to as coefficients, have been expressed as a function of corrected rotational speed N. That process results in a number of sub-coefficients depending on the type of function. The propagation of the coefficients with respect to N should be captured by smooth and simple polynomials that will not give rise to ill-conditioned extrapolation affecting the accuracy of the targeted optimization. Each coefficient is expressed as a polynomial function of corrected rotational speed as expressed in the generic form

$$g(N) = g_1 N^i + \cdots + g_i N + g_{i+1} \tag{6}$$

where g is one of map's coefficients, with i denoting the order of the polynomial function. For instance, in the second approach, the coefficient a_{π_c} is expressed

$$a_{\pi_c}(N) = a_{\pi_{c_1}} N^3 + a_{\pi_{c_2}} N^2 + a_{\pi_{c_3}} N + a_{\pi_{c_4}} \tag{7}$$

as a 3^{rd} order polynomial with a total number of 4 sub-coefficients. In case of the second fitting approach, where all the remaining coefficients $(a_{\pi_c}, b_{\pi_c}, \theta_{\pi_c}, a_{\eta_c}, b_{\eta_c}, \theta_{\eta_c})$ are expressed as a function of the speed, as seen in Fig. 4, this results in a total number of 23 sub-coefficients. The process has been performed for all three fitting approaches and the total number of sub-coefficients for each approach is tabulated in Table 1.

The total number of the sub-coefficients for the second approach is 23 as opposed to 100 required for the third approach. It can be concluded that the second approach will be implemented

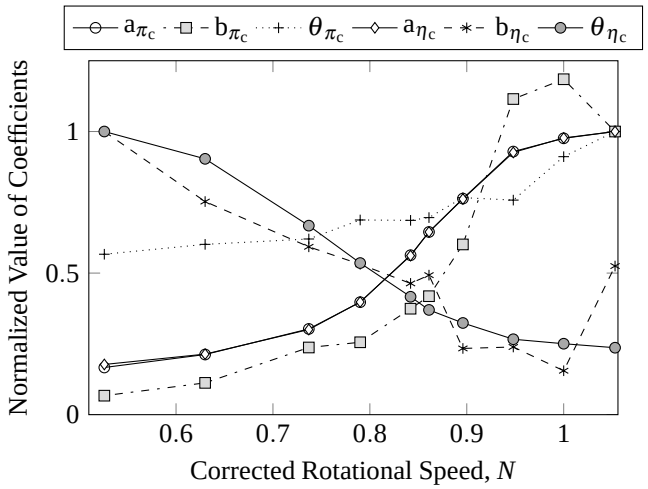

FIGURE 4: Variation of the map's coefficients w.r.t. corrected speed N.

for the engine performance prediction. The decision is justified based on the fact that this approach has a good balance between the accuracy pursued and the complexity of the mathematical equations capturing the variations of each coefficient with respect to the speed.

The above analytical process, facilitates one to mathematically control the compressor map's shape in a non-linear manner, so that the corresponding map generation method can replace simple lookup tables and/or externally linear-scaled maps in any engine model. Another advantage of the proposed fitting method is that due to the analytical equations used to represent an ellipse, the initial values of the coefficients (a, b, θ) can be easily approximated without any empirical knowledge.

2.2 Gas Turbine Engine Model

The proposed compressor map generation method has been integrated into a dynamic engine model, of a two shaft industrial gas turbine, developed in Matlab/Simulink environment and validated with PROOSIS [16]. The engine model developed consists of a compressor, a combustor, a compressor turbine and a power turbine as shown in Fig. 5. The components are represented by a set of suitable performance maps from PROOSIS, although the compressor map used is the one seen in Fig. 1.

TABLE 1: Coefficients and sub-coefficients of each approach.

Approach	Coefficients	No Sub-coefs
1	$a_{\pi_c}, b_{\pi_c}, a_{\eta_c}, b_{\eta_c}, x_0$	20
2	$a_{\pi_c}, b_{\pi_c}, \theta_{\pi_c}, a_{\eta_c}, b_{\eta_c}, \theta_{\eta_c}$	23
3	$a_{\pi_c}, b_{\pi_c}, \theta_{\pi_c}, a_{\eta_c}, b_{\eta_c}, \theta_{\eta_c}, x_0, y_0$	100

The engine simulations performed in Simulink consist of two parts, the steady state and the transient modes. Steady state simulations are performed for a fixed value of the fuel flow rate f_f and through an iterative method that guesses values of the parameters for ensuring flow and work compatibility, so that the model converges to the steady state condition. In the final converged steady state condition, values of the temperatures at the compressor, combustor, compressor turbine and the power turbine exits namely T_3, T_4, T_5, T_6 are passed onto the transient model as initial values of the corresponding integrals.

The transient simulations, based on the Inter Component Volume (ICV) method, commence from the last known converged conditions of the steady state model with the variations of the control vector f_f. During the transient response, a finite amount of time is taken for the rotor to spool up or down but the mass flow, and therefore the pressure changes inside the engine can be quite rapid. The developed engine model in Simulink, an object oriented environment, can be easily adapted to any kind of gas turbine configuration. A detailed description of the model used for this application can be found in the work [17].

2.3 Adaptive Performance Simulation

The primary aim of the adaptive performance simulations also called performance adaptation is the process of tuning the component parameters of an engine model to match a set of measurements available from a reference engine. These measurements can be either field data of a service engine or simulations of a different engine model.

The adaptive simulation algorithm, shown in Fig. 6, modifies, with respect to its input ambient and operating conditions vector **u**, the independent component characteristics vec-

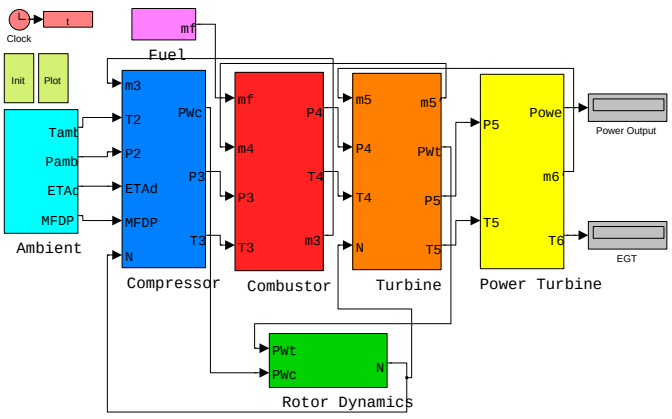

FIGURE 5: Engine model layout in Simulink.

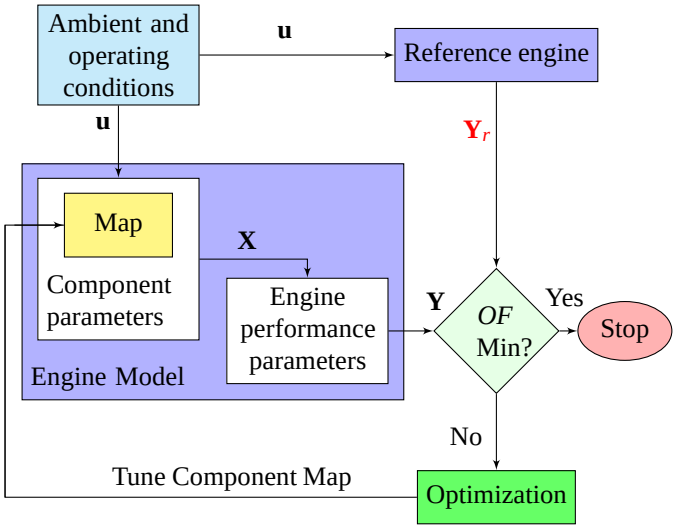

FIGURE 6: Flow chart of adaptive performance simulation.

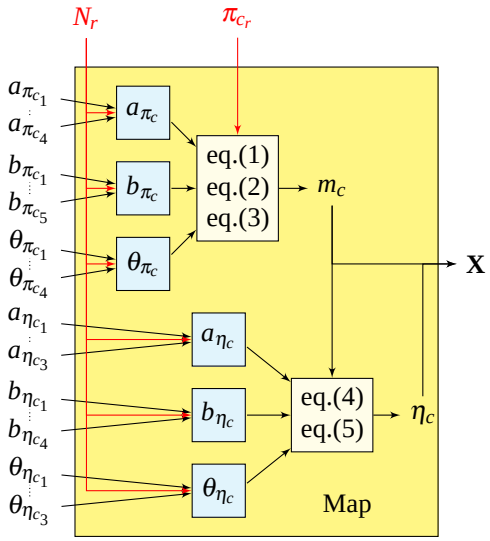

FIGURE 7: Compressor map generation.

tor $\mathbf{X} = [m_c, \eta_c]$, which includes non-measurable quantities mass flow rate and efficiency. The ambient and operating conditions vector $\mathbf{u} = [P_{amb}, T_{amb}, handle]$ consists of ambient pressure, temperature and a parameter called *handle* of the engine model acting as input to the model for engine performance simulations. Depending on the simulation approach the *handle* can be either power output, turbine entry temperature, rotational speed or any other quantity. By modifying the component vector $\mathbf{X}$ the difference between the so-called dependent measurable performance parameter vector of the engine model $\mathbf{Y}$ and the reference engine $\mathbf{Y}_r$ is minimized.

The measurable performance vectors $\mathbf{Y} = [P, T]$ and $\mathbf{Y}_r = [P_r, T_r]$ consist of engine performance measurements such as pressure and temperature at different locations of the engine. For this study, the difference between the predicted measurements $\mathbf{Y}$ and the observed measurements $\mathbf{Y}_r$ can be evaluated by means of an Objective Function (OF) defined as follows:

$$OF = \|\mathbf{A}\|_F = \sqrt{\sum_{i=1}^{q}\sum_{j=1}^{n} |\alpha_{i,j}|^2} \tag{8}$$

$$= \sqrt{\sum_{i=1}^{q}\sum_{j=1}^{n} \left| \frac{\mathbf{Y}_{i,j} - \mathbf{Y}_{r_{i,j}}}{\mathbf{Y}_{r_{i,j}}} \right|^2} \tag{9}$$

where, n refers to the total number of operating points belonging to q number of different corrected rotational speed lines. The OF in this case is the Frobenius norm of an $m \times n$ matrix A, defined as the sum of the absolute squares of its elements α, where element α is the difference between the predicted $\mathbf{Y}$ and the measurable performance vector $\mathbf{Y}_r$, divided with $\mathbf{Y}_r$. Since this adaptive performance simulation covers multiple operating points, the objective function has been modified to accommodate such a feature. The number of the measured parameters to be matched, depends on the test case itself, however for this work all of the measured parameters are used in a single grand optimization. The OF is minimized by implementing one of Matlab's built-in nonlinear unconstrained optimization algorithms [fminsearch]. The tuning of the sub-coefficients is handled by the optimizer in order to modify the shape of the map and match the engine model's predictions to the measurements produced by a reference engine.

The optimization commences with a starting value for each sub-coefficient. These initial values, determined by the fitting procedure performed earlier to a typical reference compressor map, are passed onto the compressor map generation procedure shown in Fig. 7, along with the measured corrected rotational speed N_r, in order to determine the coefficients of the map $(a_{\pi_c}, b_{\pi_c}, \theta_{\pi_c}, a_{\eta_c}, b_{\eta_c}, \theta_{\eta_c})$. Once the coefficients are calculated, the pressure ratio π_{c_r}, which is a known measurable parameter of the reference engine, is used for determining the corrected mass flow m_c by solving eqs. (1), (2), (3). The corrected mass flow m_c is then used, in the same manner as π_{c_r} before, for calculating the compressor's isentropic efficiency η_c from eqs. (4), (5). Both m_c and η_c form the independent component characteristics vector $\mathbf{X}$ which is used for the remaining thermodynamic calculations of the engine model.

Key optimization parameters such as number of iterations and tolerance criterion are specified accordingly. Once the optimization converges, the new set of sub-coefficients are passed onto the engine model. The developed algorithm can be executed both for external and internal adaptive simulations. In the case of internal adaptive simulation, the optimization of sub-coefficients

TABLE 2: Performance specification of *reference engine*.

Parameter	Value	Units
Power	3.4	MW
Pressure Ratio	10.8	
Thermal efficiency	38	%
Exh. flow rate	34	kg/s

takes place simultaneously with the iterative solving of the compatibility thermodynamic equations of the engine model.

For testing the proposed method, the *reference engine* is a similar engine model that uses the compreessor performance map, available from the literature and shown in Fig. 1. In contrast to the map generation procedure employed by the *engine model* the *reference engine* employs simple lookup tables for determining the corrected mass flow rate and the isentropic efficiency of the compressor. The test cases, that have been carried out, are described in the following section.

3 APPLICATION

The proposed adaptation approach has been implemented in a dynamic engine model developed in Matlab/Simulink environment and tested for steady state and transient conditions. As described earlier, the *reference engine* is a similar model with simple lookup tables whereas the *engine model* is utilizing the proposed map generation process. Analysis of the adaptation results and discussion of the method are provided in the results section. Performance specification of the *reference engine* is shown in Table 2.

Since the primary objective of the test cases is to evaluate the accuracy improvement of the proposed method, which incorporates the compressor map generation, the selection of inlet and outlet measurements of the compressor are crucial for the above purpose. The list of the selected measurable parameters for the adaptive performance simulation is given in Table 3.

The nominal operating point, chosen as the model design point, for this configuration is at 3.4 MW with the shaft corrected rotational speed N set as the *handle* of the engine. Three test cases are conducted. Target measurements for the first two test cases are *deck data* produced by the performance simulations of the *reference engine* with the selected compressor map implemented as a lookup table. The first two test cases assess the combined accuracy of the optimization and compressor map generation. On the other hand the objective of the third test case is to directly evaluate the elliptical fitting method proposed. This is achieved without any optimization employed, since the model is

TABLE 3: Engine performance measurable parameters.

No	Symbol	Parameter	Units
1	P_2	Compressor Inlet Pressure	Pa
2	T_2	Compressor Inlet Temperature	K
3	P_3	Compressor Discharge Pressure	Pa
4	T_3	Compressor Discharge Temperature	K
5	N	Shaft Rotational Speed	rpm

TABLE 4: Parameters of Adaptation Test Cases.

Case	Mode	Points	Iter.	Fun. Eval.	Error Tol.
1	Steady	10	10^3	2×10^3	10^{-8}
2	Transient	100	10^4	2×10^4	10^{-14}

scheduled to perform a manoeuvre not included in the the earlier adaptation cases.

In the steady state case the engine model's corrected rotational speed N is reduced from 1 down to 0.55 N. In the transient mode case, the fuel flow rate varies according to the fuel flow command schedule and the engine is decelerated and accelerated as explained in Section 4.2. The developed adaptation's accuracy is tested by generating a compressor map and tuning it through the optimizer in order to match the *deck data*. A summary of the adaptation test cases' parameters can be seen in Table 4, where the number of maximum iterations ranges from 10^3 to 10^4 with the function evaluations being twice of the former and the error tolerance range starting from 10^{-8} down to 10^{-14}.

4 RESULTS AND DISCUSSION

The proposed adaptation has been tested for steady state and transient mode conditions. The results for each test case are presented and discussed in the following subsections.

4.1 Steady State Case

The objective of the first test case is to test the accuracy of the proposed adaptation method. Having the corrected rotational speed as the *handle* of the engine, and before any optimization of the compressor map's sub-coefficients is employed, the *engine model* is not able to match the *deck data* at an appropriate level of accuracy, as seen from the dashed blue line in Figs. 8 and 9. It is observed from Fig. 8 that the error of the engine model,

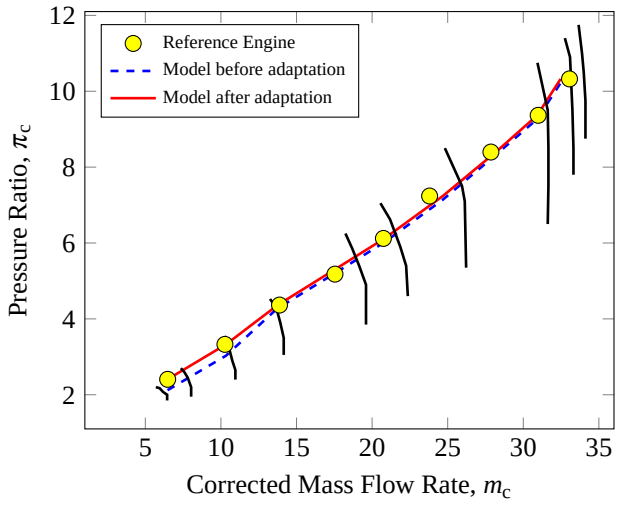

FIGURE 8: Steady state operating line.

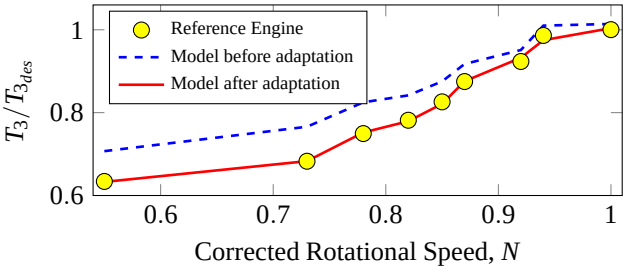

FIGURE 9: Compressor exit temperature T_3 for the steady state.

before adaptation, is increasing when the operating point is far away from the design conditions.

The above engine model's prediction error can be minimized by tuning the compressor map's sub-coefficients, which results in an optimized shape of the compressor map, tailored to match a series of target measurable parameters. Figures 8 and 9 show that the model's simulations, after adaptation, match the measurements of the reference engine at a very accurate level. The prediction error of the engine model, before and after the adaptation is employed, is shown in Fig. 10.

The compressor's discharge pressure P_3 and temperature T_3, for the adapted engine model present a maximum error in the range of -2 to 2%. On the other hand, the maximum error for the engine model, before adaptation takes place in the range of -10 to 10%. Moreover, the adapted engine model has an average error in T_3 which is equivalent to 0.05K, whereas for the un-adapted engine model this is 15K, respectively. Figure 11 shows the margin by which each one of the 23 sub-coefficients, controlling the compressor map generation process, have been modified in order to match the target measurable parameters. The normalized values, shown in Fig. 11, simply refer to the ratio between the tuned and initial sub-coefficients.

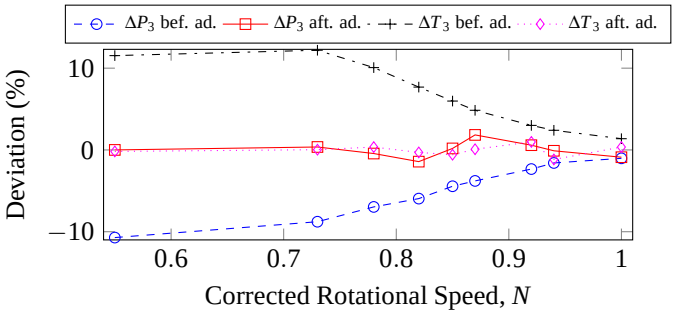

FIGURE 10: Error of measurable parameters for the steady state.

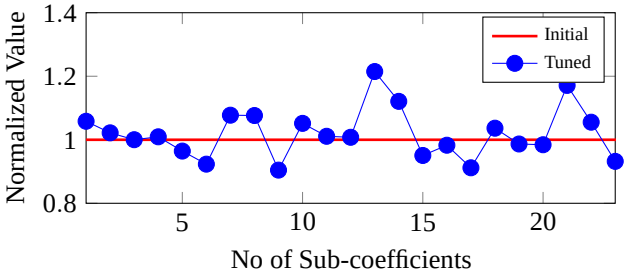

FIGURE 11: Initial and tuned map's sub-coefficients.

Another key aspect of the entire optimization process, which involves the tuning of these sub-coefficients, is its rapid convergence. For this test case where 750 iterations and a total 2000 function evaluations took place the elapsed time, when performed in a modern PC equipped with Intel's i5 quad-core processors and 4GB of RAM memory, is 0.23 sec.

4.2 Transient Mode Cases

4.2.1 Case 2

The objective of the second test case is to test the accuracy of the proposed adaptation method in transient conditions. The fuel flow rate for this test case has been scheduled accordingly and the fuel flow command is shown in Fig. 12. Simulation results for the specified fuel flow schedule of the *reference engine*, the engine model before and after adaptation are shown in Figs. 13, 14 and 15.

As seen from Figs. 13, 14 and 15 the engine model, before the adaptation takes place, is not in a good agreement with the *reference engine* as both measurable parameters T_3 and P_3 are not estimated accurately.

In order to match the measurable parameters during the tran-

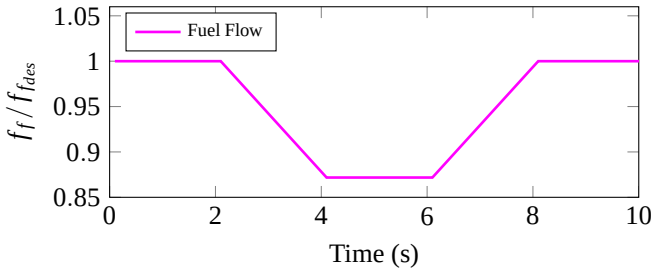

FIGURE 12: Fuel flow schedule during transient response.

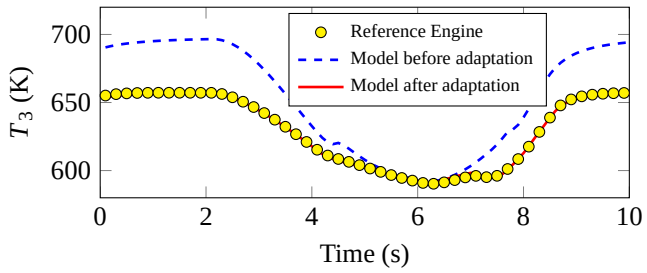

FIGURE 13: Compressor exit temperature T_3 during transient response.

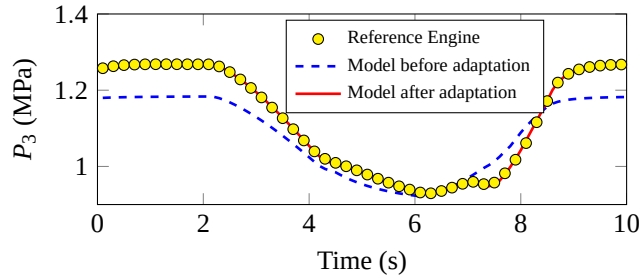

FIGURE 14: Compressor exit pressure P_3 during transient response.

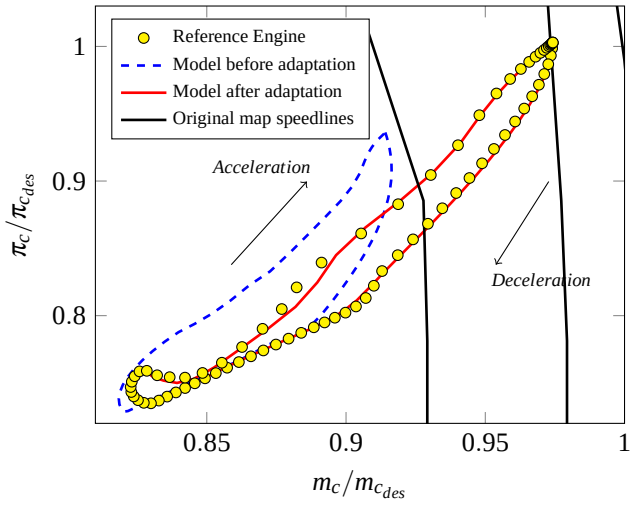

FIGURE 15: Transient trajectories on compressor characteristic map.

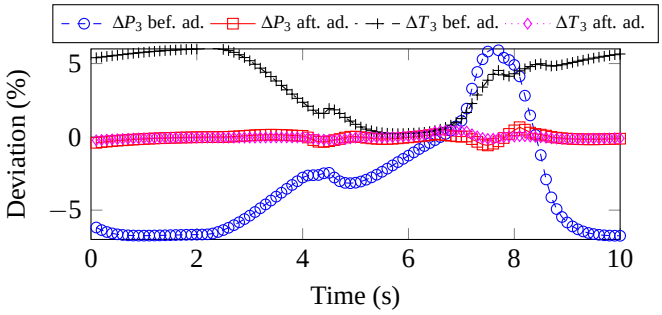

FIGURE 16: Error of measurable parameters during transient response.

sient behavior, the engine model has been adapted by employing the compressor map generation method. A total of 100 discrete operating points have been used for the adaptation. The process converged after 5000 iterations, 20000 function evaluations with the elapsed CPU time of 0.8 sec. The engine model after adaptation provides an accurate match to the *reference engine* and is capable of following the transient response as seen from the acceleration and deceleration trajectories in Fig. 15.

Figure 16 shows the prediction error of the measurable parameters for the transient test case. The deviations in compressor's discharge pressure ΔP_3 and temperature ΔT_3, for the adapted engine model are in the range of -0.6 to 0.7% . On the other hand the maximum error for the engine model, before the adaptation takes place, is in the range of -5 to 5%. For instance the adapted engine model has an average error in T_3 which is equivalent to 0.2K whereas for the un-adapted engine model this is 15K, respectively.

4.2.2 Case 3

The objective of the third test case is to test the accuracy of the proposed elliptical fitting method in transient conditions. To filter out the advantageous accuracy improvement provided by the optimization, the model performs a different transient manoeuvre that has not been included in the earlier adaptation test cases. The engine model uses the last set of optimized subcoefficients from test case 2, and follows a different fuel flow schedule. Any deviations in the prediction of the measurable parameters emphasize the effectiveness of the elliptical curve fitting employed for generating the compressor map. The fuel flow schedule and the measurable parameters for this test case are shown in Figs. 17,

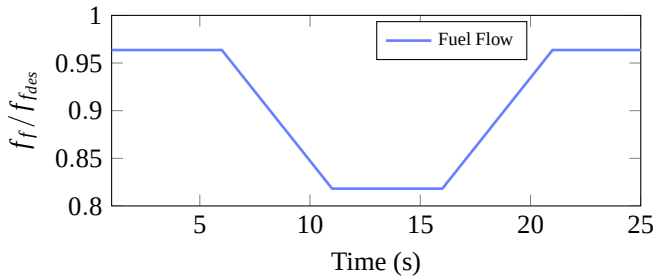

FIGURE 17: Fuel flow schedule for transient Case 3.

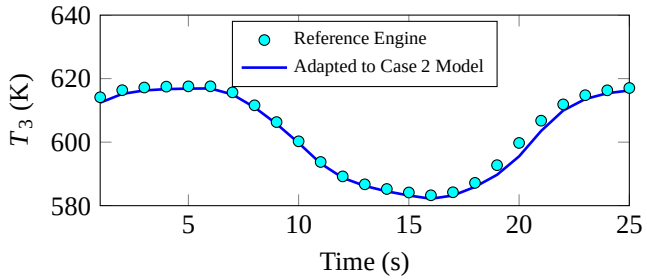

FIGURE 18: Compressor exit temperature T_3 during transient Case 3.

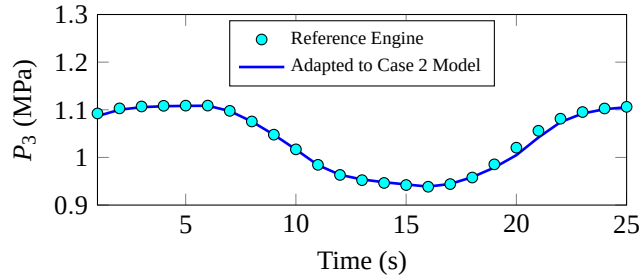

FIGURE 19: Compressor exit pressure P_3 during transient Case 3.

18 and 19.

It is noticed that the predictions of the engine model are in good agreement with the *reference engine* for a different manoeuvre without employing the optimization method. The deviation of the measurable parameters in this case is in the range of -2 to 0.6% and is more evident in the last acceleration part of the test as seen in Fig. 20.

Test cases 1 and 2 corroborate the adaptive modeling process used, and test case 3 evaluates the accuracy of the elliptical-curve modeling approach for providing good off-design prediction. The developed compressor map generation method, when coupled with the nonlinear unconstrained optimization al-

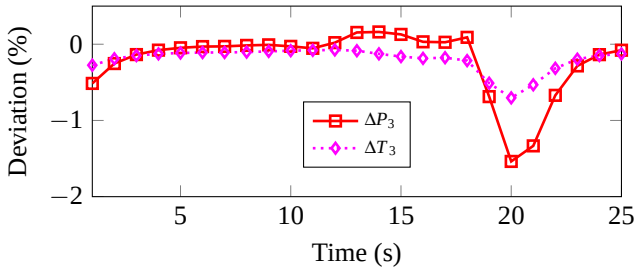

FIGURE 20: Error of measurable parameters during transient Case 3.

gorithm, facilitates an accurate and fast prediction of a gas turbine's performance at steady state and transient conditions. This is achieved by employing multi-point performance adaptation which is integrated in a dynamic engine model that is developed in Simulink/Matlab. This novel advanced adaptation method has an improved accuracy which is critical to gas path diagnostics and prognostics. Other strong features of the developed method is its wide range of accurate application, fast convergence of the optimization algorithms and its ability to capture nonlinear behavior of the gas turbines with a single set of compressor map coefficients.

This adaptation method is a useful tool for progressively refining an engine model based on multiple sets of engine test data at off-design steady state and transient conditions. All the strong features of this adaptation method emphasize the promising prospect of its application to model-based gas turbine performance diagnostics, a task that the authors are currently engaged in.

5 CONCLUSIONS

In this paper, an efficient compressor map generation method is introduced that aims to improve the accuracy of gas turbine performance prediction at steady state and transient conditions. The map coefficients, from the map generation procedure, are optimized by a nonlinear algorithm in order to match the targeted measurements of a reference model, with a compressor map available from literature, working at off-design steady and transient modes. The proposed method deals effectively with the nonlinear behavior of gas turbines away from the nominal operating points by tuning the compressor's map shape.

Application of the developed approach to a two shaft industrial gas turbine engine model demonstrates the following. In comparison with an engine model, that has not utilized any performance adaptation method, our proposed strategy shows the effectiveness that the compressor map has on the prediction accuracy of the engine models adaptive capability. The built-in nonlinear optimizer employed in this adaptation is effective in minimizing the prediction errors by adapting the compressor

maps. The computational time for a typical 10 steady operating points adaptation case is approximately 0.2 sec for 2000 function evaluations and 750 iterations and an average prediction error of 0.15%. Similarly for the transient conditions and 100 points the elapsed CPU time and prediction error are 0.8sec and 0.1%, respectively. Our proposed adaptive performance method is a useful tool for progressively refining an engine model based on multiple sets of reference engine test data at steady state and transient off-design conditions. The improved accuracy and efficient computational nature of this method is transferrable to model-based diagnostics. Therefore, the implementation of our proposed method to any gas turbine performance simulation, or condition monitoring and diagnostic tool could provide better information of gas turbine engines and aid their users to make an informed judgment for managing efficiently their gas turbine assets, increasing their availability and reducing the maintenance costs.

REFERENCES

[1] Saravanamuttoo, H., and MacIsaac, B., 1983. "Thermodynamic model for pipeline gas-turbine diagnostics". *J. Eng. Gas Turbines Power*, **105**(4), October, pp. 875–884.

[2] Zhy, P., and Saravanamuttoo, H., 1992. "Simulation of an advanced twin-spool industrial gas turbine". *J. Eng. Gas Turbines Power*, **114**(2), April, pp. 180–186.

[3] Kurkze, J., 1996. "How to get component maps for aircraft gas turbine performance calculations". In Proceedings, Vol. **1** of *ASME Turbo Expo*, Birmingham, UK. Paper 96-GT-164.

[4] Miste, G. A., and Benini, E., 2012. "Improvements in off-design aeroengine performance predictions using analytic compressor map interpolation". *Int. J. Turbo Jet-Engines*, **29**(2), June, pp. 69–77.

[5] Jones, G., Pilidis, P., and Curnock, B., 2002. "Extrapolation of compressor characteristics to the low-speed region for sub-idle performance modelling". In Proceedings, Vol. **2** of *ASME Turbo Expo 2002: Power for Land, Sea, and Air*, pp. 861–867. Paper No GT2002-30649.

[6] Sethi, V., Doulgeris, G., Pilidis, P., Nind, A., Doussinault, M., and Cobas, P., 2013. "The map fitting tool methodology: gas turbine compressor off-design performance modeling". *J. Turbomach.*, **135**(6), September.

[7] Kong, C., Ki, J., and Kang, M., 2003. "A New Scaling Method for Component Maps of Gas Turbine Using System Identification". *J. Eng. Gas Turbines Power*, **125**(4), November, pp. 979–985.

[8] Li, Y. G., Huang, K., Feng, X., Ghafir, M. F. A., Wang, L., and Singh, R., 2011. "Nonlinear Multiple Points Gas Turbine Off-Design Performance Adaptation Using a Genetic Algorithm". *J. Eng. Gas Turbines Power*, **133**(7), March.

[9] Kong, C., Kho, S., and Ki, J., 2004. "Component Map Generation of a Gas Turbine Using Genetic Algorithms". *J. Eng. Gas Turbines Power*, **128**(1), March, pp. 92–96.

[10] Drummond, C., and Davison, C., 2009. "Capturing the shape variance in gas turbine compressor maps". In Proceedings, Vol. **1** of *ASME Turbo Expo 2009: Power for Land, Sea, and Air*, pp. 177–186. Paper No GT2009-60141.

[11] Sieros, G., Stamatis, A., and Mathioudakis, K., 1997. "Jet Engine Component Maps for Performance Modeling and Diagnosis". *AIAA Journal of Propulsion and Power,*, **13**(5), September, pp. 665–674.

[12] Tsoutsanis, E., Li, Y. G., Pilidis, P., and Newby, M., 2012. "Part-load performance of gas turbines: Part 1 a novel compressor map generation approach suitable for adaptive simulation". In Proceedings, Vol. **1** of *ASME 2012 Gas Turbine India Conference*, pp. 733–742. Paper No GTINDIA2012-9580.

[13] Tsoutsanis, E., Li, Y. G., Pilidis, P., and Newby, M., 2012. "Part-load performance of gas turbines: Part 2 multi-point adaptation with compressor map generation and ga optimization". In Proceedings, Vol. **1** of *ASME 2012 Gas Turbine India Conference*, pp. 743–751. Paper No GTINDIA2012-9581.

[14] Yu, Y., Chen, L., Sun, F., and Wu, C., 2007. "Neural-network based analysis and prediction of a compressor's characteristic performance map". *Applied Energy*, **81**(1), January, pp. 48–55.

[15] Ghorbanian, K., and Gholamrezaei, M., 2009. "An artificial neural network approach to compressor performance prediction". *Applied Energy*, **86**(7), July, pp. 1210–1221.

[16] PROOSIS, 2013. *Propulsion Object-Oriented Simulation Software*, 5.2 ed. Empresarios Agrupados, A.I.E. (EA), Madrid. See also URL `http://www.proosis.com/`.

[17] Tsoutsanis, E., Meskin, N., Benammar, M., and Khorasani, K., 2013. "Dynamic performance simulation of an aeroderivative gas turbine using the matlab simulink environment". In Proceedings, Vol. **4** of *ASME 2013 International Mechanical Engineering Congress and Exposition*.

[18] Klapproth, J., Miller, M., and Parker, D., 1979. "Aerodynamic development and performance of the cf6-6/lm2500 compressor". In Proceedings, Vol. **1** of *4th International Symposium on Air Breathing Engines*.

[19] Zachos, P., Aslanidou, I., Pachidis, V., and Singh, R., 2011. "A sub-idle compressor characteristic generation method with enhanced physical background". *J. Eng. Gas Turbines Power*, **133**(8), April.

ACKNOWLEDGMENT

This publication was made possible by NPRP grant No.4-195-2-065 from the Qatar National Research Fund (a member of Qatar Foundation). The statements made herein are solely the responsibility of the authors.